

MARINTEK

Norwegian Marine Technology
Research Institute

Postal address:
P.O.Box 4125 Valentinlyst
NO-7450 Trondheim, NORWAY

Location:
Marine Technology Centre
Otto Nielsens veg 10

Phone: +47 7359 5500
Fax: +47 7359 5776

<http://www.marintek.sintef.no>
Enterprise No.: NO 937 357 370 MVA



MARINTEK REPORT

TITLE

VIVANA - Theory Manual
Version 3.4

AUTHOR(S)

Carl M. Larsen, Kyrre Vikestad, Rune Yttervik, Elizabeth
Passano and Gro Sagli Baarholm

CLIENT(S)

Joint Industry Project

FILE CODE MT51 F01-049	CLASSIFICATION Unrestricted	CLIENTS REF.	
CLASS. THIS PAGE	ISBN	PROJECT NO. 516419	NO. OF PAGES/APPENDICES 37/1
REFERENCE NO. T:\Prosjekt\PS1\516419_VIVANA\manuale r\release 3.4\VIVANA - Theory Manual P		PROJECT MANAGER (NAME, SIGN.) Halvor Lie <i>Halvor Lie</i>	VERIFIED BY (NAME, SIGN.) Carl M. Larsen <i>Carl M. Larsen</i>
REPORT NO. 516419.02.01	DATE 2005-03-01	APPROVED BY (NAME, POSITION, SIGN.) Terje Nedreliid, Div. Manager <i>Terje Nedreliid</i>	

ABSTRACT

This is the theory manual for VIVANA.

VIVANA is an FEM based program for prediction of vortex induced vibration, fatigue damage and drag amplification of slender marine structures in current. The current must be constant in time, but may vary along the structure. The analysis method is based on empirical data for hydrodynamic coefficients. An iterative procedure in frequency domain is applied for the dynamic analysis.

The program is linked to the more general riser analysis program RIFLEX.

KEYWORDS	ENGLISH	NORWEGIAN
GROUP 1	Hydrodynamics	Hydrodynamikk
GROUP 2	Fatigue	Utmatting
SELECTED BY AUTHOR	Vortex induced vibration	Virvel induserte vibrasjoner
	Dynamics	Dynamikk
	Risers	Stigerør

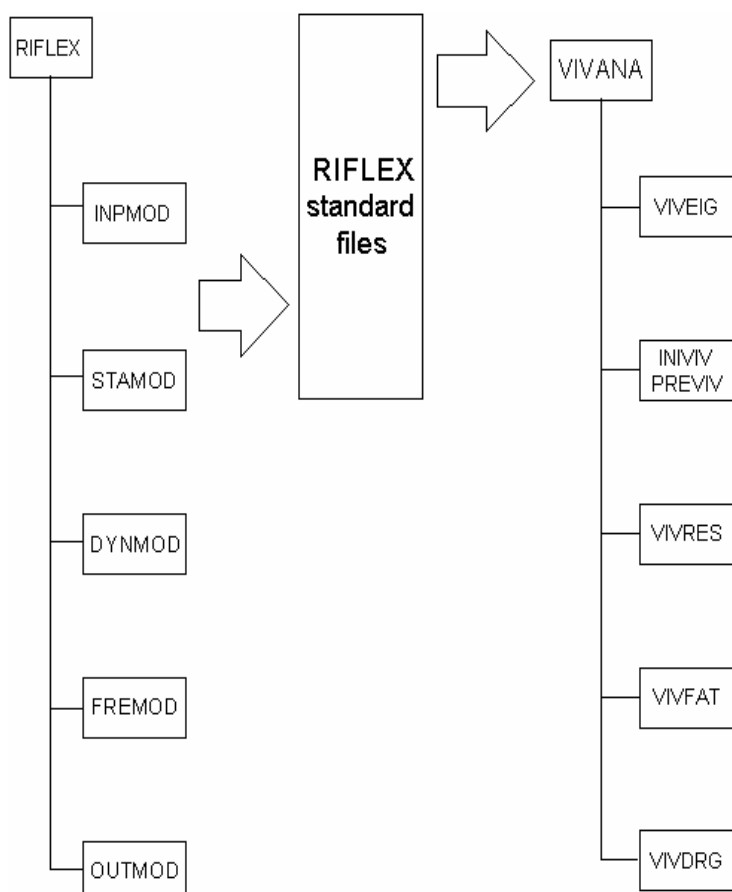
TABLE OF CONTENTS

1. Introduction	3
2. Method Overview	5
2.1 Analysis procedure; step by step	5
2.2 Solving the dynamic equilibrium equation	6
3. Initial Calculations	8
3.1 Calculation of key parameters	9
4. Excitation Parameters	13
4.1 Free oscillation and forced motion tests	13
4.2 Excitation parameters in VIVANA	18
5. Calculation of Response Frequencies	21
5.1 Basic assumptions	21
5.2 Iteration scheme	22
6. The Lift Coefficient Model	24
6.1 Default lift coefficient model	24
6.2 General lift coefficient model	26
6.3 VIV suppression devices modeling limitations	28
7. The Damping Model	29
7.1 Structural damping or relative damping	29
7.2 Model for still water, low and high reduced velocities	29
7.2.1 Venugopal Damping Model	29
7.2.2 Damping using lift curves	30
7.3 Hydrodynamic damping	31
8. Fatigue Analysis	33
9. Drag Amplification	36
References	37
APPENDIX A: Correction of non-dimensional frequency for actual Strouhal number	38

1. INTRODUCTION

The purpose of the computer program VIVANA is to calculate the response of a slender beam structure excited by vortex shedding due to a current profile. This response type is often referred to as vortex-induced vibration (VIV). VIVANA is not a complete analysis program in the sense that it is a stand-alone program that can be applied without any support from other programs. VIVANA requires that the description of structure and its static shape is available on a specific file format. In its standard implementation, VIVANA is linked to the analysis program system RIFLEX (RIFLEX Theory Manual, 1995) as shown on Figure 1.1 . RIFLEX can handle a large variety of slender marine structures such as tensioned and flexible risers, anchor lines, umbilicals, tendons, pipeline during installation and free spanning pipelines. Such structures may hence also be analysed by VIVANA.

Figure 1.1 The overall structure of VIVANA and RIFLEX



A complete VIV analysis consists of:

An initial RIFLEX analysis using the INPMOD (system modeling and environment data) and STAMOD (non-linear static analysis) modules.

The VIVEIG module computes normal modes and eigenfrequencies.

Some initial key parameters are calculated in INIVIV and an initial VIV evaluation is carried out in PREVIV.

The VIVRES module carries out the dynamic response analysis according to the method described herein.

The VIVFAT module carries out a fatigue analysis based on the results from VIVRES, and VIV amplified drag coefficients are calculated in VIVDRG.

An updated static analysis may be carried out by a second use of STAMOD where magnified drag coefficients are introduced. This type of analysis will require a special input file for RIFLEX STAMOD, which is described in the RIFLEX User's Manual.

Note that RIFLEX can handle complex structural systems in 3 dimensions and arbitrary current profiles including variation of current direction with water depth. The present VIVANA version is, however, limited to handle structures that consist of one main line only (no branching) and that in its initial configuration is found in one plane. The current profile must be unidirectional and attach the structure in its main plane or perpendicular to this plane.

2. METHOD OVERVIEW

2.1 Analysis procedure; step by step.

The analysis method is based on a three dimensional (3-D) finite element formulation that in principle may take any 3-D effects into account. The element theory is described in the RIFLEX Theory Manual (1995). A brief outline of the analysis procedure is given in the following.

Step 1. Static analysis

The static shape of the structure needs to be found. The procedure will depend on the actual system and how it is modeled in RIFLEX, cf. the RIFLEX Theory Manual.

Step 2. Eigenvalue analysis

The eigenfrequencies and mode shapes of the structure are found. Added mass is initially applied as for a non-responding riser in still water according to data given by the user. The results will be given in terms of discrete eigenvectors ϕ_i and associated eigenfrequencies ω_i (rad/s) or f_i (Hz). A sufficient number of eigenvalues will be found so that all possibly active frequencies can be found when considering the maximum vortex shedding frequency along the structure.

Step 3. Identification of possible and dominating excitation frequencies

A subset of all calculated eigenfrequencies will define the complete set of possibly active eigenfrequencies. Added mass under VIV conditions will, however, become different from the still water case as applied for the initial eigenvalue analysis. Hence, iterations must be performed for each frequency candidate in order to find a set of possible response frequencies. The iteration has converged when there is consistency between the modified eigenfrequency and modified added mass distribution. Each response frequency candidate will be associated to an excitation zone, and the dominating response frequency will be identified among the candidates according to the theory described herein.

Step 4. Analysis of the response at the dominating frequency

The frequency response method is used to calculate the dynamic response at the dominating frequency identified in step 3. The user may also specify which frequency that should be selected as the dominating response frequency. The analysis applies an iteration that converges when the response is in accordance with the non-linear models for excitation and damping. Both local response amplitude and phase are considered in this iteration.

Step 5. Response analysis for other frequencies than the dominating frequency

In case of a strongly sheared profile the result from Step 4 may show an excitation zone for the dominating frequency that does not cover the total length of the structure. Consequently excitation may take place at other frequencies in zones outside the identified zone. A similar analysis as for Step 4 must now be carried out for each frequency, but the excitation zone will now become the original zone for the new frequency with a reduction according to the zone taken by the more dominating frequencies. Note that if the user decides to apply another

frequency than the program as the dominating response frequency, the resulting response will be influenced since another frequency will be given the privilege of occupying its total potential excitation zone.

Step 6. Post-processing of results

Post-processing includes fatigue analysis and calculation of amplified drag coefficients.

In addition to the analysis procedure outlined above, the program will present results from an evaluation of the actual riser's performance regarding VIV, see Section 4.

As mentioned before it is possible to proceed to a Step 7 that will carry out an updated static analysis with amplified drag forces according to the results from VIVANA. It is also possible to apply the RIFLEX DYNMOD module to carry out an improved dynamic analysis by using intermediate results from VIVANA in a non-linear time domain model. This option is not available in the standard VIVANA program. For further details, see Larsen et.al. (2004)

2.2 Solving the dynamic equilibrium equation.

Vortex induced vibration (VIV) is assumed to take place at discrete frequencies. Laboratory tests and full-scale measurements support this assumption. A certain frequency bandwidth of the response may be seen, in particular for cases where the response is dominated by mode orders above 10. However, the discrete frequency assumption is still applied in the proposed model. Note that the response may include more than one frequency at the same time, but the present version of the program does not account for any non-linear interaction between frequencies.

In the case of discrete frequencies the response may be calculated by using finite elements and the frequency response method. The equation of dynamic equilibrium is written

$$M\ddot{r} + C\dot{r} + Kr = R \quad (1)$$

The external loads will be harmonic, but loads at all degrees of freedom are not necessarily in phase. It is convenient to describe this type of load by a complex load vector with harmonic time variation

$$R = X e^{i\omega t} \quad (2)$$

where X is a complex vector and ω is the load frequency. The response vector will also be given by a complex vector and a harmonic time variation. Hence we have

$$r = x e^{i\omega t} \quad (3)$$

By introducing the hydrodynamic mass and damping matrices, dynamic equilibrium can now be expressed as:

$$-\omega^2(M_S + M_H)x + i\omega(C_S + C_H)x + Kx = X_L \quad (4)$$

where

M_S Structural mass matrix

M_H Hydrodynamic mass matrix, function of ω and the local flow speed

C_S Structural damping matrix

C_H Hydrodynamic damping matrix, function of amplitude, ω and flow speed

X_L Excitation force vector, which is zero in the damping regions and always in phase with the local velocity in the excitation region. The local load is a function of response amplitude, ω and flow speed

In this equation it is necessary to define the hydrodynamic damping matrix, and also the load vector as functions of the response vector. Iteration is hence needed when solving this equation. Note that the response frequency is fixed during this iteration, cf. step 3 in the analysis procedure. The iteration will identify a response shape and amplitude that gives consistency between the response level and applied coefficients.

3. INITIAL CALCULATIONS

The initial information related to hydrodynamic coefficients needed for application of the present theory is the Strouhal number for all cross sections valid for a non-vibrating structure, and the added mass for all cross section valid in still water. Any variation along the structure of these parameters is allowed since the finite element method is applied for structural modeling and solving the eigenvalue and dynamic response problem.

A key issue is to identify the conditions for vortex induced vibrations to occur, and to define limitations for current speed to excite a particular frequency. Three different terms regarding excitation will be applied in this manual:

The excitation zone is a zone along the structure consisting of one continuous part or a number of segments where the vortex shedding process will feed energy into the vibrating structure. Outside this zone there must be a damping zone where an identical amount of energy is dissipated. If an excitation zone covers the entire riser length (uniform current profile), there must be an energy balance within the zone found by inspecting the response amplitude and lift coefficient variation. Negative lift coefficients will normally be found where response amplitudes are large.

The excitation zone for a given current profile will be linked to a particular response frequency identified as an eigenfrequency found for an added mass distribution consistent with this frequency and the current profile. It will be shown that the extension of this zone can be defined from the response frequency, current profile, Strouhal number and riser diameter. Parameters like reduced velocity or mass ratio will not have any influence on the extension of the excitation zone once the response frequency is found.

The excitation frequency bandwidth is defined as the maximum and minimum value for a non-dimensional frequency parameter that will give excitation. The definition of this bandwidth is based on results from experiments with a cylinder under forced motions perpendicular to a constant flow. The excitation frequency bandwidth is universal in the sense that the non-dimensional values are fixed and not dependent on any case specific parameters.

The reduced velocity excitation range is defined as maximum and minimum values for the reduced velocity that can excite a single degree of freedom system. The system is defined by its eigenfrequency in still water, diameter and dry mass, and may be understood as a two-dimensional cylinder in a spring or a specific modeshape of a flexible cylinder in uniform flow. The response frequency will always appear as an eigenfrequency found by considering the actual added mass, and the frequency will vary for varying reduced velocity.

It will be shown that this excitation range will increase for decreasing mass ratio for the cylinder. This excitation range will not enter the definition of the excitation zone for a structure, but indicate whether a structure can respond with a particular frequency in a given uniform current profile. The purpose of introducing the reduced velocity excitation range is not to support a response analysis, but to understand the dynamic behavior of a structure under lock-in

conditions. Note that the reduced velocity in this work always is defined with reference to the eigenfrequency in still water and not to the actual oscillation frequency.

One objective of this section is to give a clear understanding of these terms and the parameters that are used to define them. It is also an ambition to describe the link between reduced velocity as a parameter to present results from freely oscillating cylinders and the non-dimensional frequency parameters used for cylinders with forced motions.

3.1 3.1 Calculation of key parameters

Initially some key parameters based on input values will be computed. All parameters will be linked to an element in the finite element model. The position of the midpoint of element number i is assumed to be defined by a co-ordinate z_i . The user must provide the following parameters:

Environmental data

Current profile	$U(z_i)$	[m/s]
Water temperature (global)	T	[°C]

The water temperature is needed since the kinematic viscosity of water - and hence also the Reynolds number - is strongly dependent on temperature. Reynolds number will be used to calculate the local Strouhal number.

Riser data (defined for each finite element along the riser)

Volume correct diameter, applied to define added mass and buoyancy	$D_V(z_i)$	[m]
Hydrodynamic diameter, applied to define Strouhal number, Reynolds number, non-dimensional frequency amplitude ratio	$D_H(z_i)$	[m]
Mass of riser including content	$m(z_i)$	[kg/m]
Added mass coefficient for still water	C_a	[-]

To be calculated

Reynolds number	$Re(z_i) = \frac{U(z_i)D_H(z_i)}{\nu(T)}$	(5)
-----------------	---	-------

where $\nu(T)$ is the temperature dependant kinematic viscosity, found from Faltinsen (1990)

Strouhal $St(z_i)$ number can be defined in three different ways (confer also input description)

The user can specify a fixed Strouhal number (independent of Re) valid for each riser segment
The built-in curve for Strouhal number as function of Re can be used, see Figure 3.1.
The user may specify an alternative curve for Strouhal number.

Note that some segments in a riser may apply alternative 1 with different fixed values, while others may apply different curves. All Strouhal numbers should be referred to a fixed (non-vibration) cross section.

Vortex shedding frequency, fixed cross section

$$f_v(z_i) = \frac{U(z_i)}{D_H(z_i)} \cdot St(z_i) \quad (6)$$

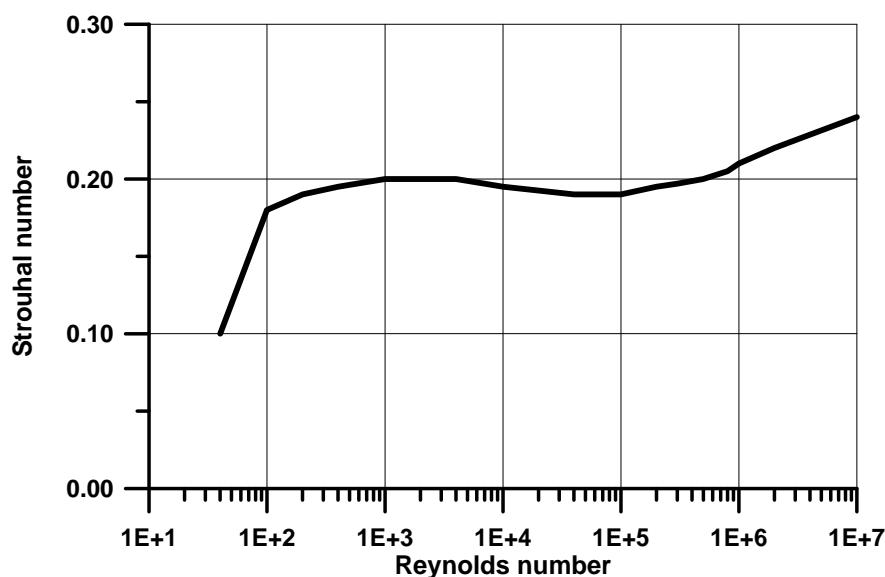
Having access to the mass and stiffness matrices VIVANA calculates the eigenfrequencies and associated eigenvectors (modeshapes) valid for still water by using the given added mass distribution:

Eigenfrequencies	f_{0j}	$[H_z]$	$j = 1, 2, \dots N$
Eigenvectors	ϕ_j	$[-]$	$j = 1, 2, \dots N$

Figure 3.2 and Figure 3.3 show how the above-mentioned parameters are presented by VIVANA.

Figure 3.1 Built-in curve for Strouhal number as function of Reynolds number

Strouhal number vs. Reynolds number, VIVANA response model



The built-in curve for Strouhal number as function of Reynolds number is taken from Blevins (1990). A curve for rough cylinder is chosen. This curve is assumed to be the best possible alternative for the present use of Strouhal number, namely to link the response frequency and vortex shedding frequency. Experience indicates that even if the vortex shedding frequency for a fixed, smooth cylinder might be significantly higher in the critical flow regime than what is indicated by the curve, the response frequency will drop to a level more like the rough cylinder case.

Figure 3.2 Initial parameters

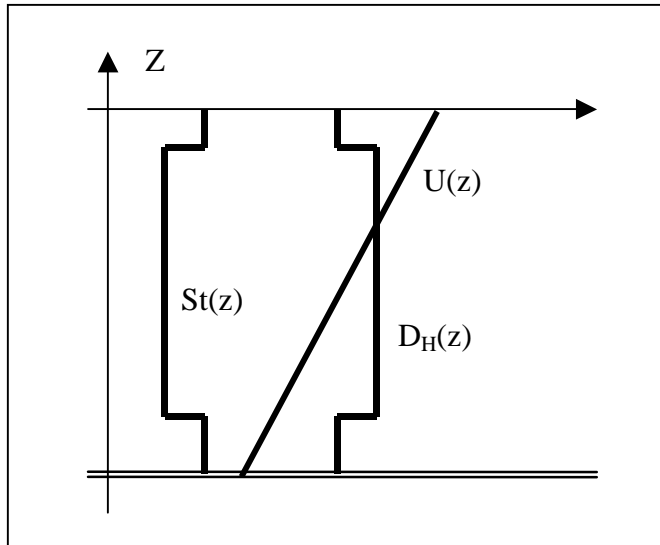
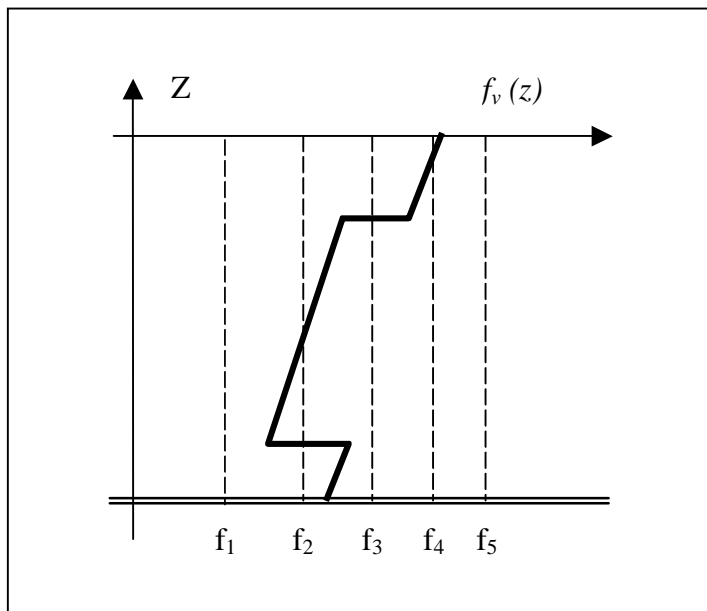


Figure 3.3 Map of vortex shedding frequency and eigenfrequencies



4. EXCITATION PARAMETERS

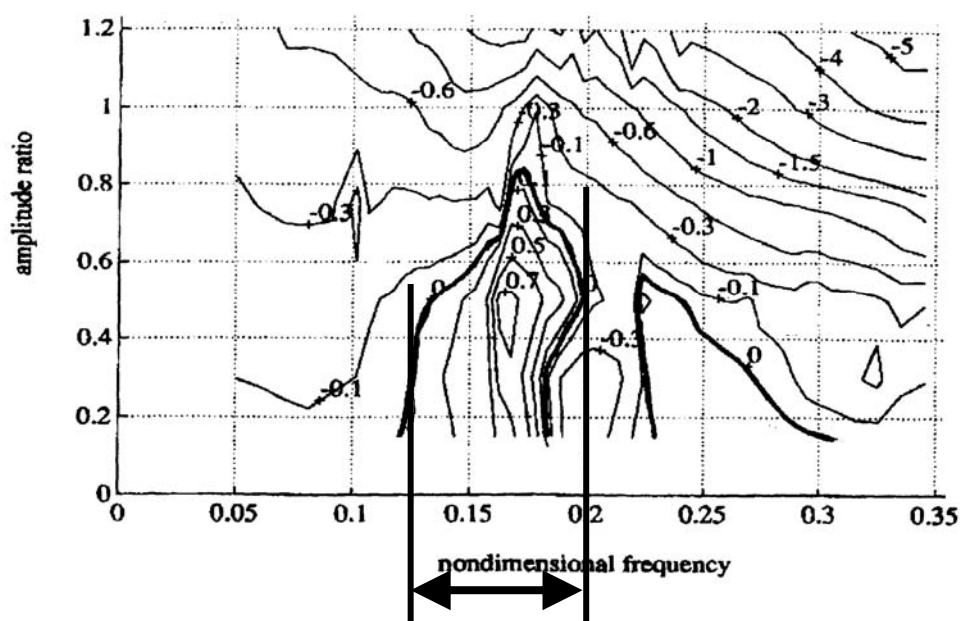
4.1 Free oscillation and forced motion tests

The purpose of this section is to describe how experiments with a cylinder with forced motions are related to experiments with a freely oscillating cylinder and thereby explains the theory behind the VIV evaluation presented by VIVANA.

Gopalkrishnan (1993) has published results from forced motions experiments, while results from experiments with an elastically supported cylinder are reported by Vikestad (1998). Gopalkrishnan's results from forced motion tests in uniform flow are presented in terms of contour plots for the lift coefficient C_L and added mass coefficient C_a as functions of non-dimensional frequency and amplitude ratio, see Figure 4.1 and 4.2. C_L defines the force in phase with the cylinder velocity, and will hence give an excitation force if it is positive. A negative C_L means that the lift force will give damping. C_a is the added mass coefficient that defines the hydrodynamic force in phase with the cylinder acceleration. This coefficient may of course also have negative and positive values. The interval that is indicated on Figure 4.1 will be commented in Section 4.2

The $C_L = 0$ contour line defines the ideal lock-in condition simply because zero lift force means that there is no energy transmission between the cylinder and the fluid – which also is the case for an undamped cylinder under steady state lock-in. By drawing this contour line in the added mass diagram, we can identify C_a under lock-in condition. Vikestad has shown that these results are very close to what he found from his experiments with a freely oscillating cylinder with very low mechanical damping.

Figure 4.1 Contour plot of the lift coefficient in phase with the velocity, forced harmonic motions. From Gopalkrishnan (1993).

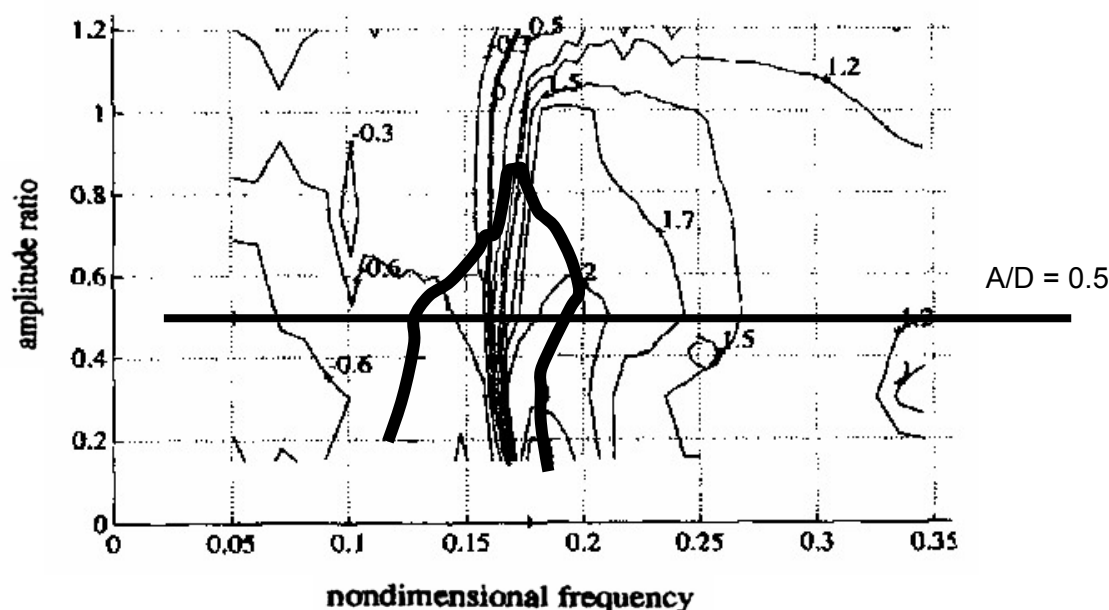


The non-dimensional frequency applied in Gopalkrishnan's plots is defined by:

$$\hat{f} = \frac{D_H}{U} \cdot f_{osc} \quad (7)$$

where f_{osc} is the oscillation frequency for the forced cylinder motions.

Figure 4.2 Contour plot of the added mass coefficient, forced harmonic motions, Gopalkrishnan (1993). The frequency/amplitude combinations that give $C_L=0$ are also shown.



Along the $C_L = 0$ curve we have ideal lock-in condition. This means that the forced motion frequency must be identical to the free oscillation frequency, which also is the eigenfrequency of the cylinder when taking the actual added mass into account. This observation helps us to establish a relationship between the non-dimensional frequency parameter and the reduced velocity parameter that normally is applied when presenting results from a freely oscillating cylinder, see also Vikestad (1998).

The oscillation frequency for a cylinder with dry mass M_D supported by a spring with stiffness k is given by:

$$f_{osc} = \frac{1}{2\pi} \sqrt{\frac{k}{M_D + \rho VC_a}} \quad (8)$$

where C_a is the actual added mass coefficient. The reduced velocity U_R is linked to the eigenfrequency in still water, f_o , found for added mass equal to C_{a0} . Hence we have:

$$U_R = \frac{U}{D_H \cdot f_o}, \quad f_o = \frac{1}{2\pi} \sqrt{\frac{k}{M_D + \rho VC_{a0}}} \quad (9)$$

By combining Eq 7, 8 and 9 we have

$$\hat{f} = \frac{1}{U_R} \sqrt{\frac{M_D + \rho V C_{a0}}{M_D + \rho V C_a}} \quad (10)$$

and

$$f_{osc} = f_0 \sqrt{\frac{M_D + \rho V C_{a0}}{M_D + \rho V C_a}} \quad (11)$$

In the general case we may define a mass ratio by relating the dry mass to added mass in still water, C_{a0} . For Gopalkrishnan's experiments we have all reason to believe that $C_{a0} = 1$. We can therefore introduce the mass ratio defined as:

$$\bar{M} = \frac{M_D}{\rho V C_{a0}} = \frac{M_D}{\rho V} \quad (12)$$

and rewrite the equations for the general and special case:

$$\hat{f} = \frac{1}{U_R} \sqrt{\frac{\bar{M} + 1}{\bar{M} + \frac{C_a}{C_{a0}}}} = \frac{1}{U_R} \sqrt{\frac{\bar{M} + 1}{\bar{M} + C_a}} \quad (13)$$

$$f_{osc} = f_0 \sqrt{\frac{\bar{M} + 1}{\bar{M} + \frac{C_a}{C_{a0}}}} = f_0 \sqrt{\frac{\bar{M} + 1}{\bar{M} + C_a}} \quad (14)$$

If C_{a0} is different from 1.0 we may apply the results from Gopalkrishnan's tests as a base for scaling. The ratio C_a/C_{a0} will then become identical to C_a , now understood as a value taken from Figure 4.1.

In order to illustrate the implications of these equations we will present Gopalkrishnan's data for $C_L = 0$ by using reduced velocity instead of non-dimensional frequency as parameter. Figure 4.3 defines the $C_L = 0$ curve in terms of corresponding values for A/D and \hat{f} , while added mass along this curve must be taken from Figure 4.2. Figure 4.4 shows the motion amplitude as function of U_R for a set of mass ratio values.

Figure 4.3 Combinations of non-dimensional amplitude and frequency that give $CL = 0$.

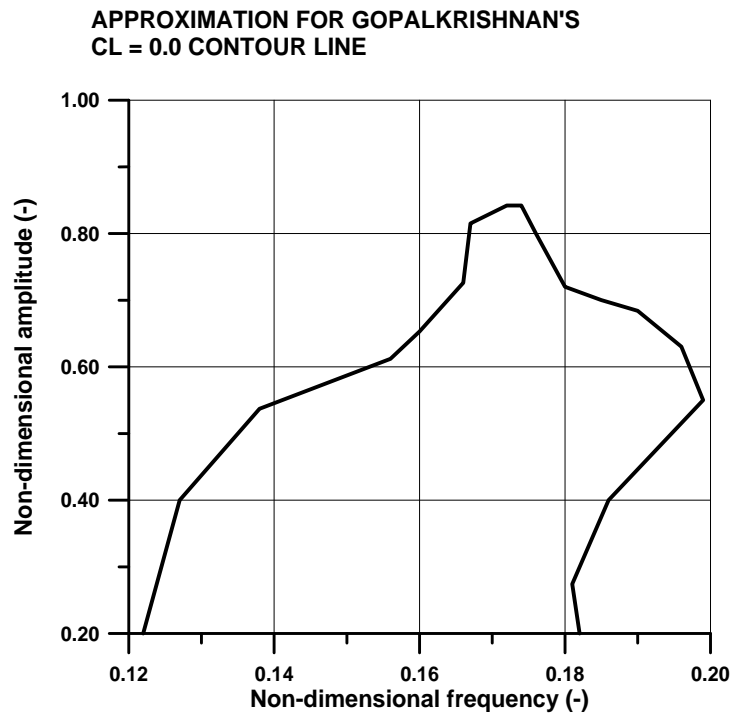
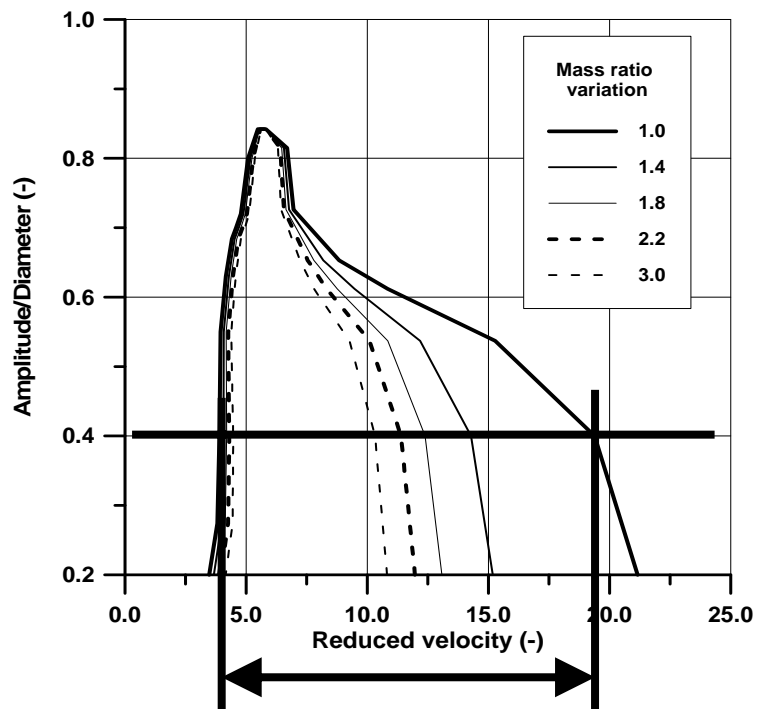
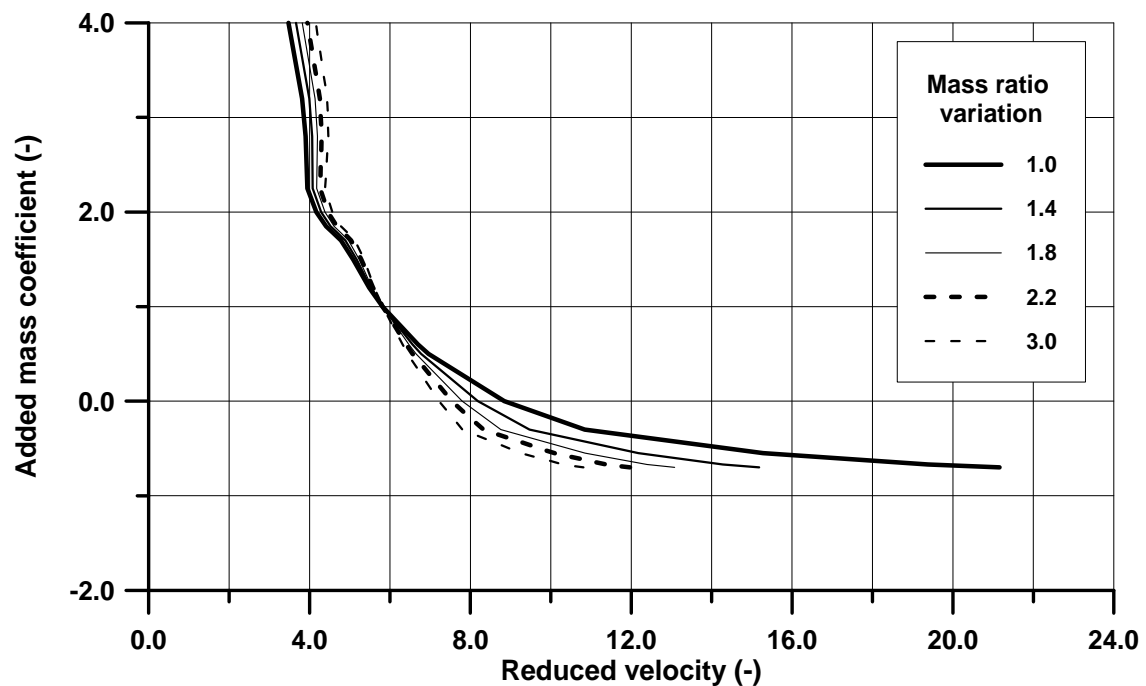


Figure 4.4 Amplitude as function of reduced velocity and mass ratio, valid for $C_L = 0$. Excitation range for mass ratio = 3 indicated



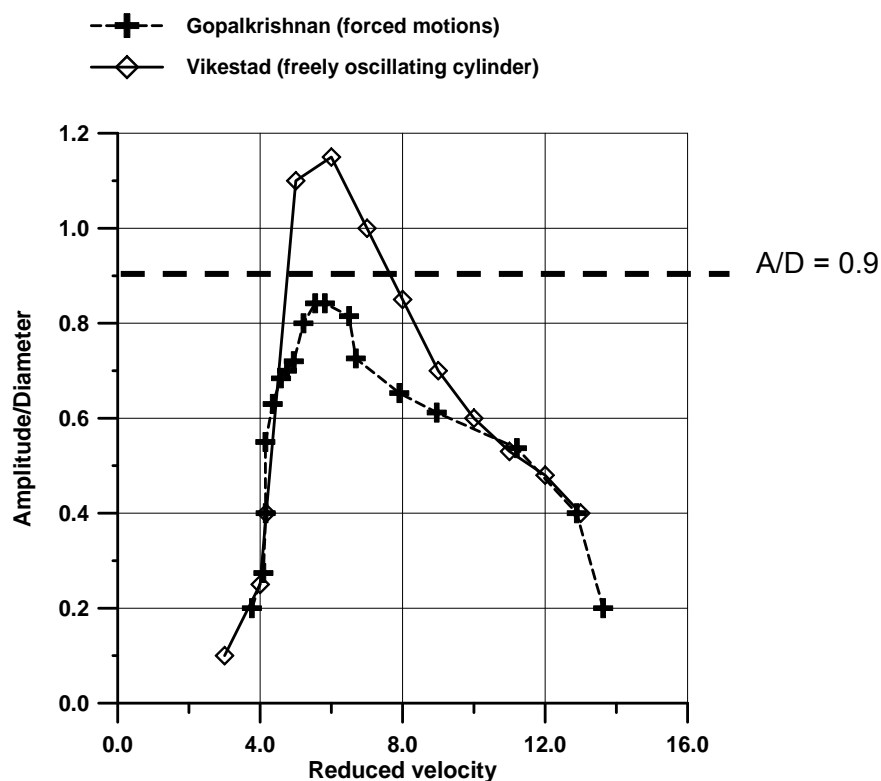
Similar curves for the added mass coefficient are shown on Figure 4.5. Both sets of curves illustrate the importance of mass ratio when using U_R as parameter. It is important to note that the oscillation frequency varies according to Eq. 13 along the reduced velocity axis and that this variation is linked to the mass ratio.

Figure 4.5 Added mass as function of reduced velocity and mass ratio, valid for $C_L = 0$.



Use of Eq. 13 makes it also possible to make a direct comparison of results from Vikestad and Gopalkrishnan, which is shown on Figure 4.6. The curves show amplitude ratios for ideal lock-in and are seen to agree very well for low and high reduced velocity values. However, Vikestad's freely oscillating cylinder has a significantly larger response than Gopalkrishnan's forced oscillation tests indicate for $5.4 < U_R < 10$. This discrepancy is hard to understand, but might be caused by the large freedom Vikestad's cylinder has to adjust its response to external forces. This is in contrast to the cylinder with forced motions that is programmed to follow a pure sinusoidal motion. The large discrepancy within the most interesting reduced velocity range is the main reason for not using results from forced motions as the only support for a response model. The broad, dotted line on Figure 4.6 indicates an A/D value of 0.9, which will be used as a reference for the present lift force model. This will be further commented in Chapter 6.

Figure 4.6 Comparison between Vikestad's and Gopalkrishnan's tests.



4.2 4.2 Excitation parameters in VIVANA

The curves presented in Section 4.1 can now be applied to define the excitation terms mentioned in the introduction of Section 3.

The excitation frequency bandwidth is defined from Figure 4.1. The area within the $C_L = 0$ contour line is the area with positive lift force, and hence the excitation area in the $A/D - \hat{f}$ space. The frequency bandwidth is seen to depend on the A/D ratio. One may, however, take a pragmatic approach and define an excitation bandwidth valid for moderate amplitude values. In this study we have selected to define the excitation bandwidth as follows:

$$\begin{aligned} \hat{f}_{\min} &= 0.125 \\ \hat{f}_{\max} &= 0.20 \end{aligned} \quad (15)$$

This definition is independent on the reduced velocity, but must be corrected for variations in Strouhal number. If we assume that the excitation zone is determined by the ratio between the actual oscillation frequency and the vortex shedding frequency for a fixed cylinder, we have to correct these boundaries. In the program we keep the boundaries constant, but redefine the non-dimensional frequency as shown in Appendix A.

From Figure 4.1 it is seen that there is a second area with zero and positive lift for higher values of the non-dimensional frequency. This area will lead to excitation at lower flow velocities than the primary excitation range. The effect will normally be irrelevant for marine risers since stresses from VIV at the first eigenfrequency and mode will be very low, and the shift from lower to higher modes will take place at the same flow speed irrespective of the second excitation range. However, for free spanning pipelines one may prefer to include this area in order to predict correct response at low flow speed. This can be obtained by specifying a user defined excitation range, see Section 5.4.1 in VIVANA User's manual. The lift coefficient data shown in Figure 6.2 covers both the primary and secondary excitation ranges.

The reduced velocity excitation range can be defined from Figure 4.4 since we here have the response amplitude as function of the reduced velocity. It is obvious that the excitation range must depend on the mass ratio, and should be linked to a selected response amplitude level. Again we have taken a pragmatic approach. The reduced velocity excitation range is defined as the variation of U_R that will give a response amplitude larger than $0.4 D$. As seen from Figure 4.4 the range is not sensitive to the selected response level on the low U_R side, but to some extent on the higher side.

We can now apply Eq. (4.7) to define this range since we know added mass and non-dimensional frequency and added mass at the boundaries. Hence we have:

$$U_{R,\min} = \frac{1}{\hat{f}_{\max}} \sqrt{\frac{\bar{M} + 1}{\bar{M} + \frac{C_{a,\max}}{C_{a0}}}} \quad \text{where } \hat{f}_{\max} = 0.186 \text{ and } C_{a,\max} = 2.8$$

$$U_{R,\max} = \frac{1}{\hat{f}_{\min}} \sqrt{\frac{\bar{M} + 1}{\bar{M} + \frac{C_{a,\min}}{C_{a0}}}} \quad \text{where } \hat{f}_{\min} = 0.127 \text{ and } C_{a,\min} = -0.67$$

(16)

If we use the modified reduced velocity equations given in Appendix A that account for varying Strouhal number, these boundaries depend on the mass ratio only. Note that this excitation bandwidth is not applied as a parameter in the VIVANA response model.

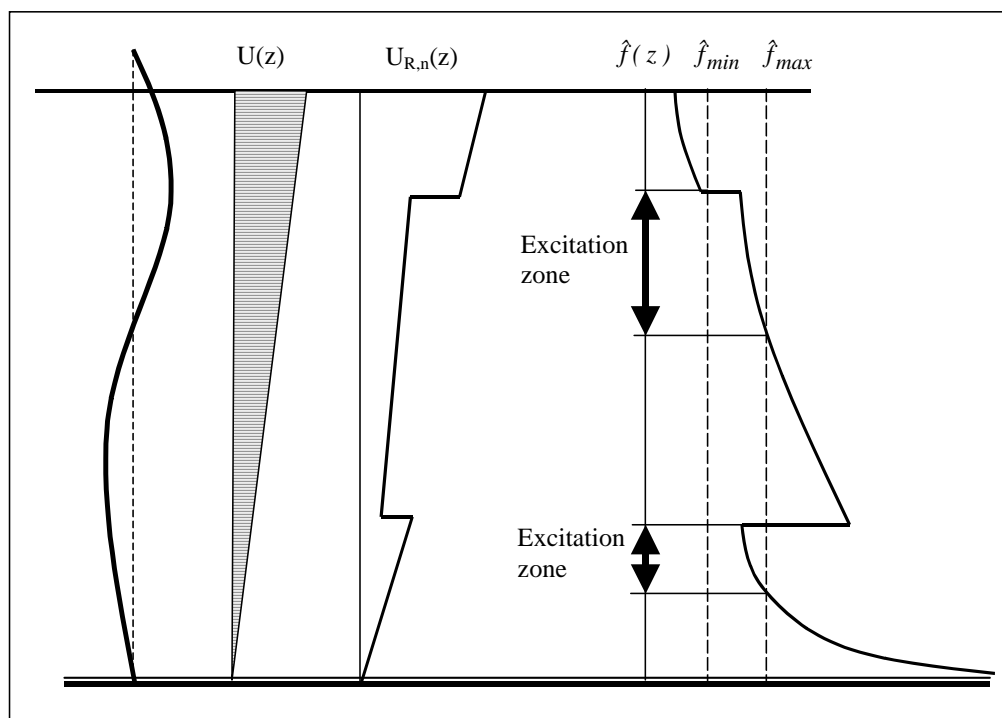
The excitation zone for a structure with a known oscillation frequency in sheared current must be linked to the excitation frequency bandwidth and not to the reduced velocity range. This is obvious if we keep in mind the physics behind the definition of the reduced velocity excitation range. This range is linked to a specific cylinder's ability to adjust its eigenfrequency towards the vortex shedding frequency by adjusting its added mass. In VIVANA we need to define the excitation zone for a predetermined oscillation frequency, meaning that no adjustment will take place any more. Figure 4.7 shows how the excitation zone will be defined.

Formally we may of course define the reduced velocity profile from Eq. 16:

$$U_{R,n}(z) = \frac{U(z)}{D_H(z)f_{0,n}} \quad (17)$$

This will give a reduced velocity profile valid for an eigenfrequency $f_{0,n}$, see Figure 4.7. However, we can not relate the variation of $U_{R,n}$ along the riser to the variation of U_R in a two-dimensional test. The reason is simply that the oscillation frequency for the riser at lock-in is constant along its length, but in the section test we have a frequency variation for varying flow speed – determined from added mass variation and hence linked to the mass ratio. The reduced velocity excitation range can therefore help us to understand how a riser will respond if we have a uniform current profile with varying current speed from one time to another. This is the issue for the evaluation performed in VIVANA.

Figure 4.7 Current profile, reduced velocity, non-dimensional frequency and excitation zone.



5. CALCULATION OF RESPONSE FREQUENCIES

5.1 Basic assumptions.

The purpose of this part of the analysis is to identify all possible response frequencies when taking into account that the flow velocity, diameter, added mass and Strouhal number vary along the riser. The analysis to find the response frequencies applies the non-dimensional frequency \hat{f} as controlling parameter. Excitation and damping zones related to a specific oscillation frequency can then be defined as shown in Chapter 4.

When the structure is exposed to a current profile, added mass will change along its length, and the response frequency will be found as an eigenfrequency for this added mass distribution. However, since the added mass depends on the frequency, this distribution can not be found directly. Consistency between the frequency and added mass distribution is therefore obtained through an iteration process.

The starting point for this analysis is a set of eigenfrequencies valid for still water. The information needed to carry out this analysis can be summarized as follows:

Eigenfrequencies in still water	$f_{01}, f_{02}, \dots, f_{0N}$
Current velocity profile	$U(z)$
Hydrodynamic diameter	$D_H(z)$
Strouhal number for fixed cross section	$St(z)$
Added mass coefficient for still water	$C_{a0}(z)$

Added mass as function of the non-dimensional frequency must be established. This information is available from Figure 4.2, but the response amplitude is also used as a parameter here, which is irrelevant for the eigenfrequency iteration. It can be seen from Figure 4.2 that added mass is almost independent on the amplitude for amplitudes between 0.2 and 0.8. This observation makes it possible to eliminate the amplitude as parameter and establish a unique relationship between frequency and added mass.

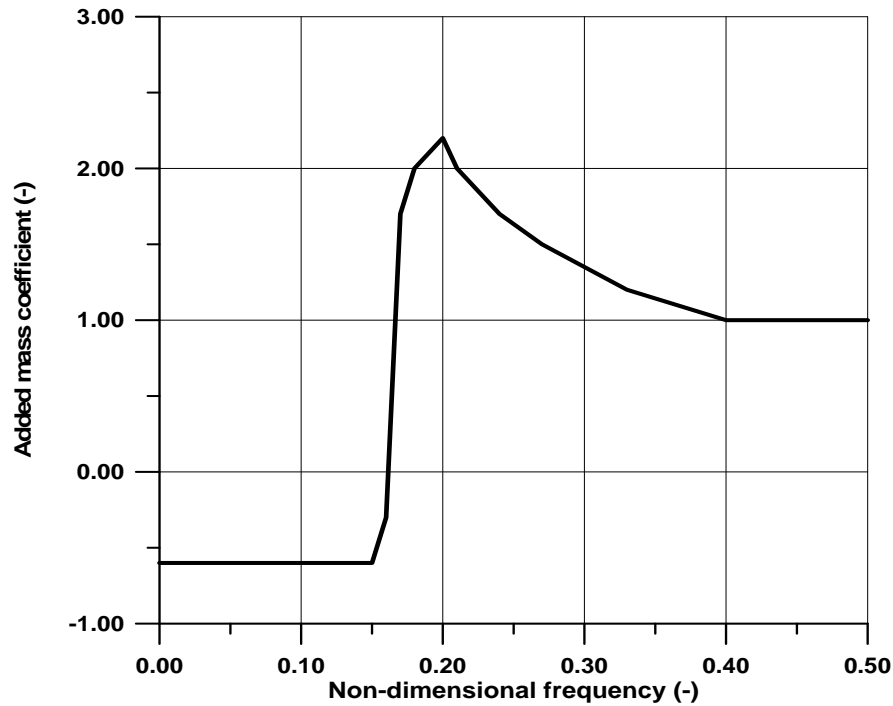
Figure 5.1 shows the variation of added mass if a constant amplitude line ($A/D = 0.5$) in Figure 4.2 is followed. This curve is applied in VIVANA to account for added mass variation.

As criterion to limit actual eigenfrequencies among the total set of frequencies the following is applied:

An eigenfrequency f_{0i} may be modified and become a response frequency if the minimum non-dimensional frequency \hat{f}_G^{\min} found along the riser is lower than \hat{f}_{max} ; the upper excitation limit \hat{f}_{lim}^{excit} (see Chapter 4). Hence, $f_{0\ i+1}$ is the lowest eigenfrequency that will give $\hat{f}_G^{\min} > \hat{f}_{max}$, and hence bring the entire riser outside the excitation bandwidth.

Figure 5.1 Added mass as function of non-dimensional frequency

**Added mass as function of
 non-dimensional frequency
 (from Gopalkrishnan)**



5.2 5.2 Iteration scheme.

The initial situation is illustrated in Figure 5.2. For each possibly active eigenfrequency, i , the following iteration is carried out:

Assume that the response frequency is identical to the eigenfrequency:

$$f_{osc,i}^k = f_{0i}^k \quad (18)$$

k is the iteration step; here $k = 1$, meaning that f_{0i}^k is the initial eigenfrequency

Calculate the non-dimensional frequency along the riser: (See Appendix A)

$$\hat{f}_{G,i}^k(z) = \frac{f_{osc,i}^k \cdot D(z)}{U(z)} \cdot \frac{St_G}{St(z)} \quad (19)$$

Find the added mass coefficient along the riser from Figure 5.1 as a function of the non-dimensional frequency and re-calculate the added mass matrix and total mass matrix.

Solve the eigenvalue problem with the new mass matrix and identify the wanted eigenfrequency f_{0i}^{k+1} .

Convergence test:

$$|f_{0i}^{k+1} - f_{0i}^k| \leq \varepsilon \quad (20)$$

where ε is a built-in criterion for convergence that can be adjusted by the user.

If the test fails, go to 1. If the test is satisfied, go to the next step

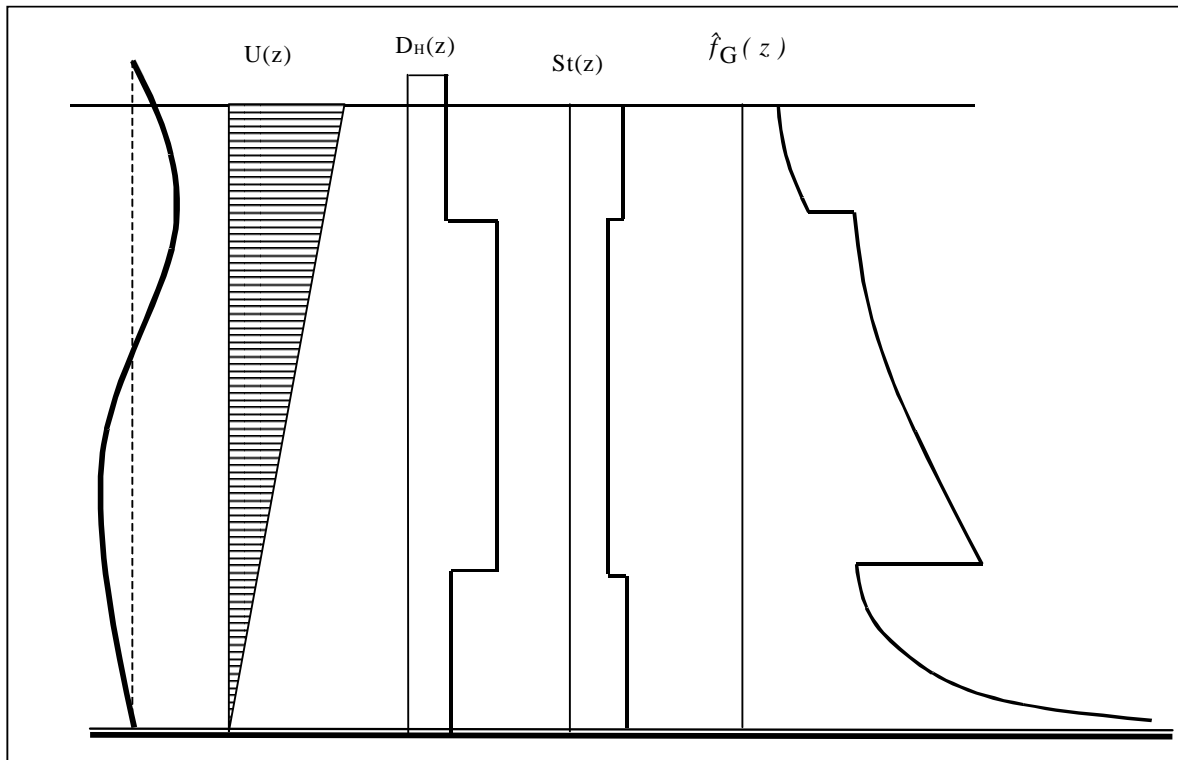
Accept f_{0i}^{k+1} as a possible response frequency $f_{osc,i}$.

Calculate the non-dimensional frequency along the riser from:

$$\hat{f}_{G,i}(z) = \frac{f_{osc,i} \cdot D(z)}{U(z)} \cdot \frac{St_G}{St(z)} \quad (21)$$

If $\hat{f}_{G,i}(z)$ is within the excitation limit for any z , the actual frequency may be excited, and the frequency needs to be further evaluated.

Figure 5.2 Riser in sheared current and key parameters.



6. THE LIFT COEFFICIENT MODEL

The lift coefficient is used in the response analysis for calculating the lift force on the cylinder. Two different ways of specifying lift coefficients are available in VIVANA. Calculation of the lift force is irrespective of how the lift coefficients are specified by the user.

Lift force is calculated for elements within the excitation zone. The excitation zone is defined by the excitation frequency bandwidth, see Section 4.2 for details. The excitation frequency bandwidth is by default [0.125, 0.2], but it is possible for the user to define his/her own excitation frequency range for any part of the cable, see Section 5.4.1. The user should never define an excitation frequency bandwidth larger than the frequency range for which lift coefficients are provided. Elements outside of the excitation zone will add damping to the system, see Section 8.2 for details.

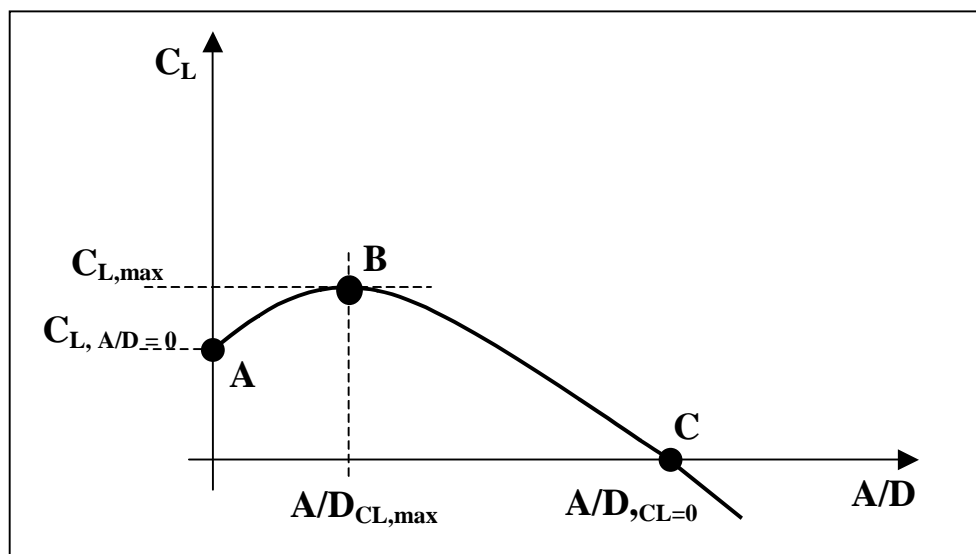
6.1 Default lift coefficient model

The default lift coefficient model in VIVANA is to a large extent based on the coefficients found by Gopalkrishnan (1993), see Figure 4.1. However, the maximum value for zero lift – corresponding to the maximum amplitude for a cylinder under lock-in condition – is significantly lower in Gopalkrishnan's tests than what was observed by Vikestad (1998), see Figure 4.6. It has therefore been considered unconservative to apply Gopalkrishnan's data directly. On the other hand, Vikestad's results for an oscillating cylinder gives a higher response amplitude than observed for flexible cylinders, see Lie et.al. (1997). It is therefore decided to apply a maximum value of 0.9D, which is illustrated in Figure 4.6. This is a pragmatic approach and could be modified if future tests give a clear indication that another value is more correct.

Figure 6.1 shows how the lift coefficient is defined in VIVANA. The coefficient is found as a function of the non-dimensional response amplitude, but the parameters that defines the curve are functions of the non-dimensional response frequency. The curve is assumed to have a maximum value (horizontal tangent) at B, meaning that AB and BC can be given as two second order polynomial when the three points A, B and C are defined. The co-ordinates of these three points are given as functions of the non-dimensional frequency, see Figure 6.2

Point A gives the lift coefficient value for zero response amplitude, $C_{L, A/D=0}$. From Figure 4.1 it is seen that Gopalkrishnan's experiments do not give C_L values for $A/D < 0.15$. and is defined from Figure 6.2. A careful extrapolation of the results is therefore carried out, and the applied values are seen in Figure 6.2. It should be noted that the response will in most cases not be significantly influenced by this value since a load at a position with low oscillating amplitude will give a small contribution to energy input.

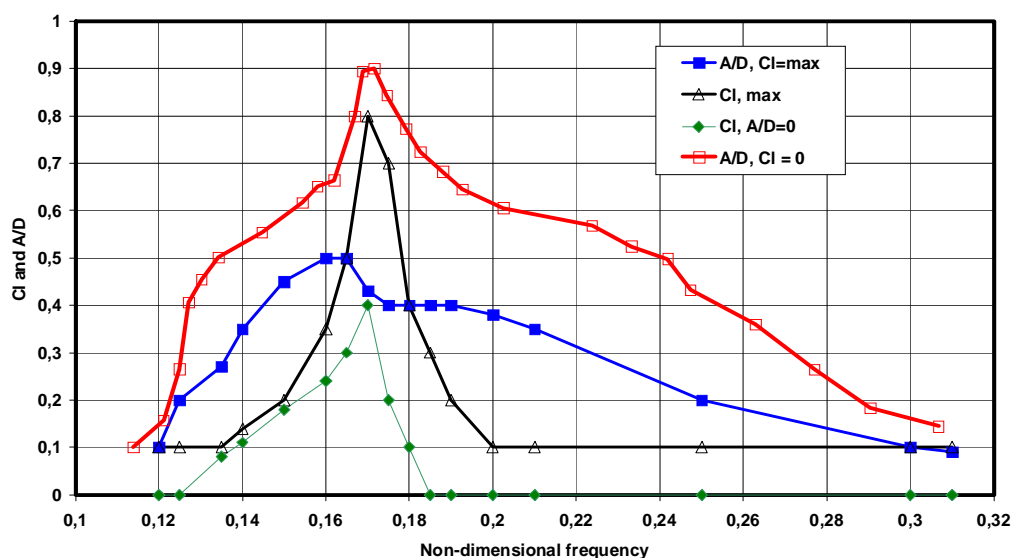
Figure 6.1 The lift coefficient model.



Point B is defined by the maximum lift coefficient and the response amplitude that gives maximum lift ($A/D_{CL,max}$). This amplitude will depend on the non-dimensional frequency and is taken as 0.5 for frequency values above 0.145, and a linear function to zero between 0.145 and 0.125, see Figure 4.1.

Point C defines the A/D value that gives zero lift for the actual non-dimensional frequency and is mainly taken from Figure 4.6. However, the data close to the peak value have been adjusted to have a maximum value of 0.9 as previously mentioned.

Figure 6.2 Definition of lift coefficients parameters

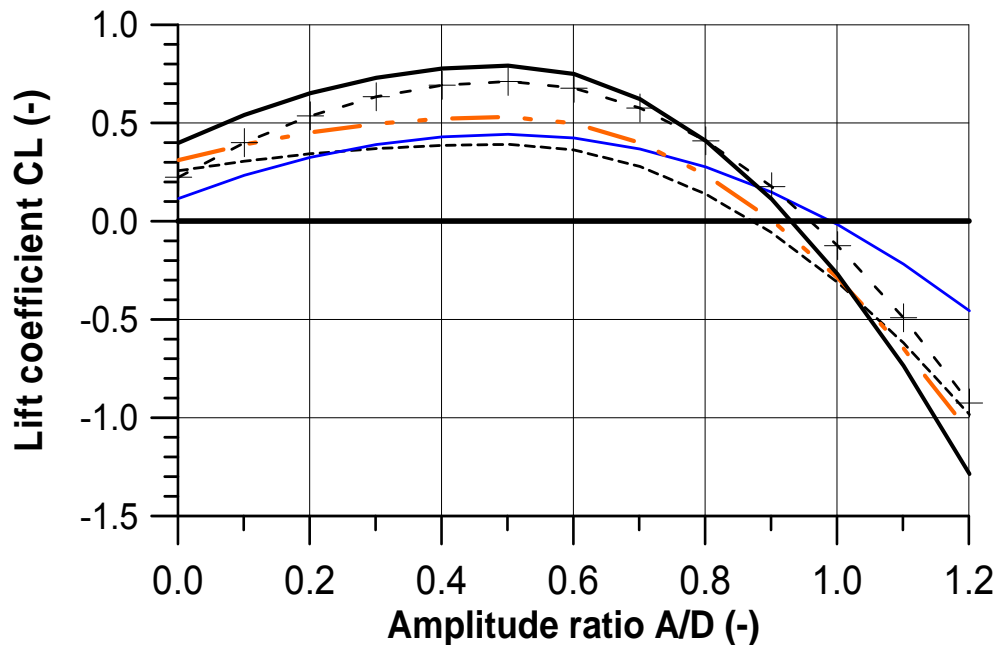


The lift coefficient curve will define damping for larger response amplitudes than $A/D_{CL=0}$ within the excitation zone. The following rules apply to define negative lift coefficients:

For larger values of A/D than $A/D_{CL=0}$, the lift coefficient is negative and found by a direct extrapolation of the quadratic curve. This approach is found to represent the values found by Gopalkrishnan with sufficient accuracy.

Examples of coefficients used in the program are shown in Figure 6.3.

Figure 6.3 Lift coefficients used in VIVANA for a set of non-dimensional frequencies.



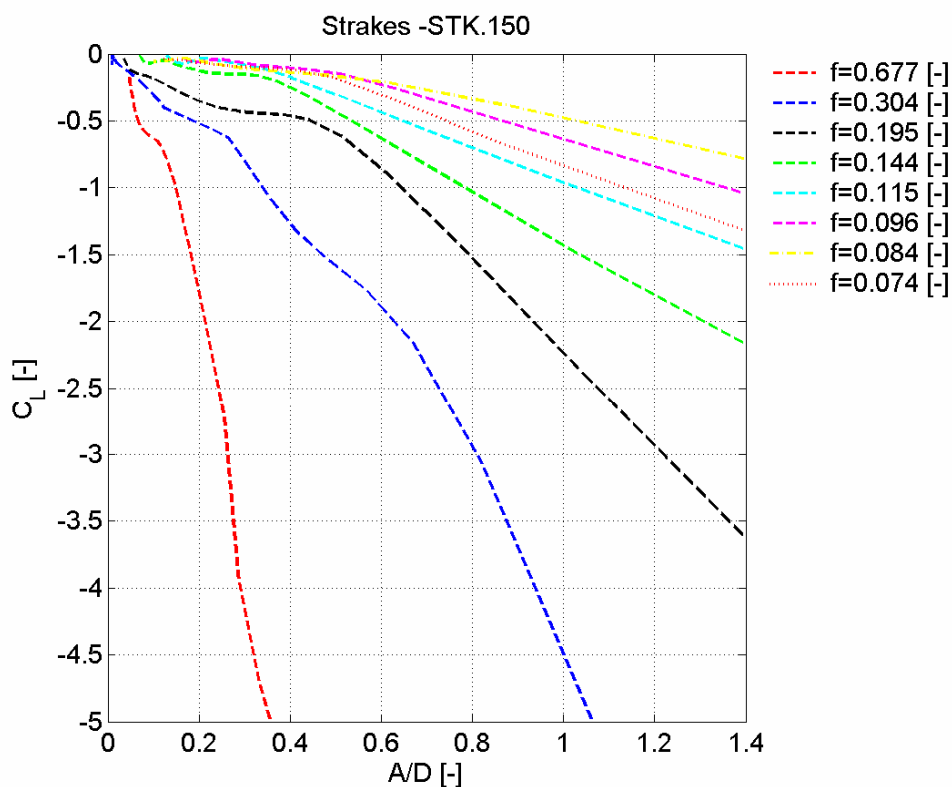
6.2 General lift coefficient model

The general lift coefficient model in VIVANA allows for easy input of model test results and results from CFD calculations. The general lift coefficient can be used to model sections with VIV suppression devices. Lift coefficients for oscillating cross-sections in cross-flow are expected to be found as tables of data as shown in Figure 6.4. The data set in Figure 6.4 can be viewed as N curves, see Figure 6.5.

Figure 6.4 Lift coefficient data from model testing and results from CFD calculations.

Strake height /D	U_{red}	A/D	C_L	fhat
0.15	1.4772	1.4638	-45.2768	0.67695084
0.15	1.4772	1.0005	-23.5147	0.67695084
0.15	1.4772	0.7666	-14.7398	0.67695084
0.15	1.4772	0.6243	-11.0215	0.67695084
0.15	1.4772	0.5212	-8.7272	0.67695084
0.15	1.4772	0.4414	-6.7043	0.67695084
0.15	1.4772	0.3795	-5.2652	0.67695084
0.15	1.4772	0.3304	-4.6772	0.67695084
0.15	1.4772	0.2877	-3.9575	0.67695084
0.15	1.4772	0.2561	-2.7208	0.67695084
0.15	1.4772	0.2331	-2.3244	0.67695084
0.15	1.4772	0.2119	-1.9861	0.67695084
0.15	1.4772	0.1940	-1.6958	0.67695084
0.15	1.4772	0.1786	-1.4439	0.67695084
0.15	1.4772	0.1654	-1.2428	0.67695084
0.15	1.4772	0.1541	-1.0754	0.67695084
0.15	1.4772	0.1443	-0.9452	0.67695084
0.15	1.4772	0.1358	-0.8445	0.67695084
0.15	1.4772	0.1282	-0.7690	0.67695084
0.15	1.4772	0.1212	-0.7142	0.67695084
0.15	1.4772	0.1148	-0.6762	0.67695084
0.15	1.4772	0.1086	-0.6505	0.67695084
0.15	1.4772	0.1027	-0.6332	0.67695084

Figure 6.5 Typical lift coefficient curves, general model.



Lift coefficients for each element within the excitation zone is found from curves like these (if the general lift coefficient model is used). Linear interpolation / extrapolation is used for finding lift coefficient for a given \hat{f} and A/D at an element node.

Negative lift coefficient will define damping; see Section 7.2.1 for further details.

6.3 VIV suppression devices modeling limitations

The theoretical model can cover cases with up to approximately 75% coverage of VIV suppression devices. For these cases the bare riser controls the VIV behavior (frequency, mode etc.)

For larger coverages the straked riser takes control of the VIV behavior. Model tests indicate a different physical behavior than for the bare controlled riser. The behavior seems to be dependent on pitch and height of the strakes. The responding frequencies and modes are generally lower.

7. THE DAMPING MODEL

7.1 Structural damping or relative damping.

The structural damping is often given as a percentage, ζ , of the critical damping, c_{cr} :

$$\bar{c} = \zeta \bar{c}_{cr} = 2\omega\zeta\bar{m} = 2\frac{\zeta}{\omega}\bar{k} \quad (22)$$

where the over-lined symbols are generalized properties. This means that the structural damping matrix for the system may be written as a fraction of either the total stiffness or the total mass matrix, whichever is more convenient.

7.2 Model for still water, low and high reduced velocities.

The damping can be calculated in two different ways in VIVANA. One option is to use Venugopal's model for still water, low and high reduced velocities, Venugopal (1996). The other possibility is to use the lift curves to calculate a damping force and to calculate the still water damping using empirical formulae.

For definition of excitation and damping regions, see Chapter 4.2.

7.2.1 Venugopal Damping Model

VIVANA uses the damping model proposed by Venugopal (1996). This model was verified by Vikestad et al. (2000). Outside the excitation regions, the damping force per unit length is found by multiplying the appropriate coefficient found below by the cross-section velocity term (dimension $[N/(m/s)/m]$):

1. Damping in still water:

$$R_{sw} = \frac{\omega\pi\rho D^2}{2} \left[\frac{2\sqrt{2}}{\sqrt{Re_\omega}} + k \left(\frac{x_0}{D} \right)^2 \right] \quad (23)$$

where $Re_\omega = \omega D^2 / \nu$. The first part corresponds to the skin friction according to Stoke's law. The second part is the pressure-dominated force. The factor k is a value found from curve fitting to be 0.25, but it may be changed if better experimental data becomes available.

2. Damping in low reduced velocity regions:

$$R_{IV} = R_{sw} + \frac{1}{2}\rho DUC_{vI} \quad (24)$$

The damping is increasing linearly with respect to the incident flow velocity. The coefficient C_{vI} was found to be 0.36 based on measurements.

3. Damping in high reduced velocity regions:

$$R_{hv} = \frac{1}{2} \rho \frac{U^2}{\omega} C_{vh} \quad (25)$$

This model is independent of the amplitude ratio. The coefficient C_{vh} was found to be 0.4 based on measurements.

If the element is in the excitation zone and the lift coefficient is negative, the damping contribution is calculated from

$$R_{cl} = -\frac{\rho \cdot D \cdot U^2 C_L}{2 \cdot \omega \cdot A} \quad (26)$$

where C_L is the lift coefficient.

7.2.2 Damping using lift curves

A riser can be partly covered with VIV suppression devices. This will imply that the lift curves and the damping on the strakes sections will vary from the lift coefficients used on the bare sections.

In Figure 7.1, a sketch of vertical riser with uniform cross section exposed to sheared current is shown. The excitation zone for a given response frequency is shown with red. The excitation zone is partly on the bare riser and partly on the sections with suppression devices. The damping on the bare riser is calculated using Venugopal's damping model, see Section 7.2.1. The damping on the upper part of the riser can be calculated using the lift curves defined for the sections with suppression devices. This implies that the lift coefficients *must* be negative for all frequencies less or larger than the two frequencies defining the excitation zone, negative for all frequencies and all (A/D) -ratios.

If the element is in the damping zone and damping from lift curves should be used or that the element is in the excitation zone and the lift coefficient is negative, the damping contribution is calculated from

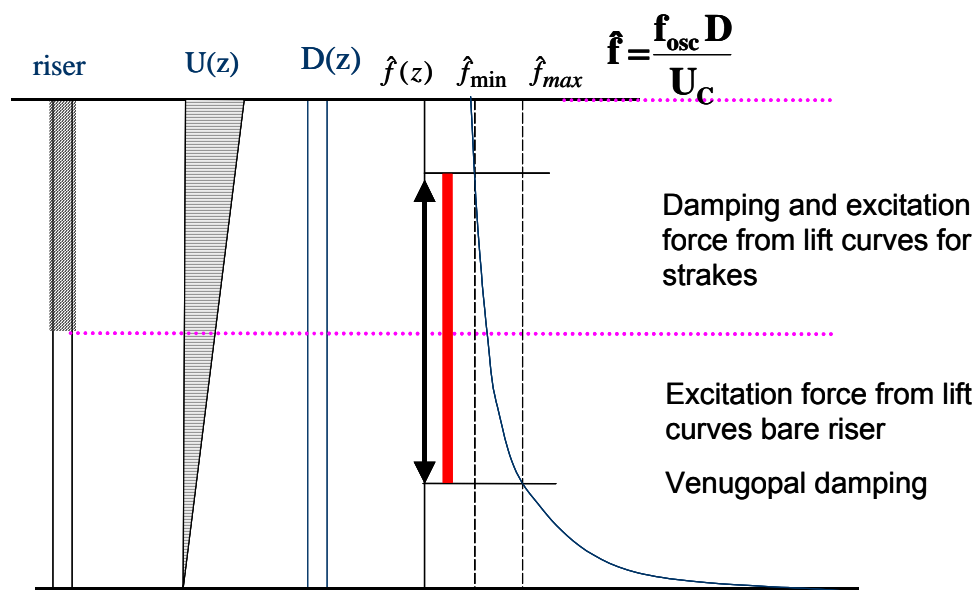
$$R_{cl} = -\frac{\rho \cdot D \cdot U^2 C_L}{2 \cdot \omega \cdot A} \quad (27)$$

where C_L is the lift coefficient.

The damping in still water is found using the still water damping coefficient c_{sw} . The scaling coefficient F_{still} must be found by using still water decay data.

$$R_{sw} = \frac{\omega\pi\rho D^2}{2} \left(1 + \left(\frac{A}{D} \right)^2 \right) F_{still} \quad (28)$$

Figure 7.1 Example on riser partly covered with strakes



The still water damping coefficient as a function of the A/D -ratio is shown in Figure 7.2 together with the data points.

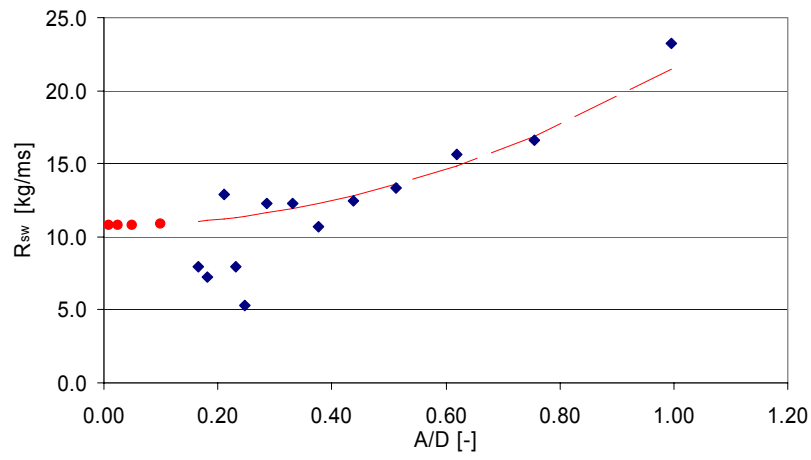
7.3 Hydrodynamic damping

The coefficients in the hydrodynamic damping matrix for an element is found in the standard FEM way:

$$c_{ij} = \int_l R(x) N_i(x) N_j(x) dx \quad (29)$$

where N denotes the shape functions for the element.

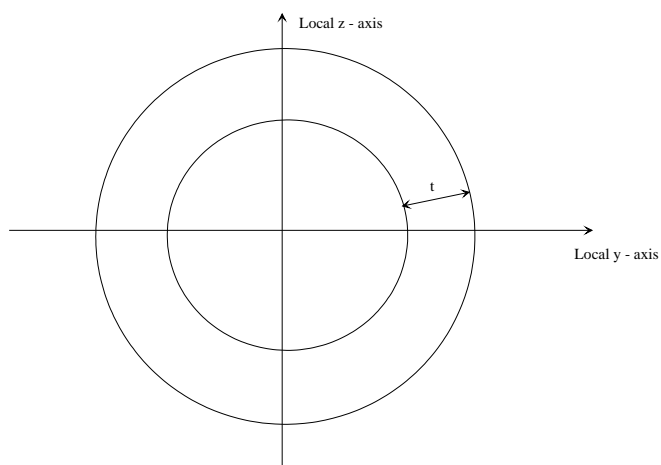
Figure 7.2 Still water damping using general lift curves.



8. FATIGUE ANALYSIS

VIVANA is able to calculate the fatigue damage in simple circular cross-sections, see Figure 8.1.

Figure 8.1 Simple circular cross-section.



When the VIV response analysis is finished we are left with N_f complex response vectors, \mathbf{x}_r , $r=1,2,\dots,N_f$. These are used in combination with the element stiffness matrices and cross section properties to arrive at time series of stress at the element ends. Stress cycles are counted by the rain flow counting method and fatigue damage is then found by Miner-Palmgren summation.

The procedure is as follows:

1. Complex vectors of element forces for all elements at all response frequencies are calculated by

$$\mathbf{s}_{r,iel} = \mathbf{k}_{iel} \cdot \mathbf{x}_{r,iel}, \quad r = 1, 2, \dots, N_f, \quad iel = 1, 2, \dots, N_{el}$$

where N_{el} is the total number of elements, \mathbf{k}_{iel} is the element stiffness matrix and $\mathbf{x}_{r,iel}$ contains the components from \mathbf{x}_r that correspond to the local degrees of freedom for the element. The dimension of $\mathbf{s}_{r,iel}$ and $\mathbf{x}_{r,iel}$ is 12, and \mathbf{k}_{iel} is 12 x 12.

2. The stress at the element ends are found as

$$\sigma_{r,jel,iend,ipt} = \mathbf{p}_{iel,ipt} \cdot \mathbf{s}_{r,jel,iend}, \quad r = 1, 2, \dots, N_f, \quad iel = 1, 2, \dots, N_{el}, \quad ipt = 1, 2, \dots, N_{pt}, \quad iend = 1, 2$$

where $\mathbf{s}_{r,iel,iend}$ is a vector of dimension 6 (the first 6 components in $\mathbf{s}_{r,iel}$ if $iend = 1$, and the last 6 component if $iend = 2$), $\mathbf{p}_{iel,ipt}$ is a vector of dimension 6 containing the cross section properties of the element, N_{pt} is the number of places on the cross section that is to be checked for fatigue.

$$\mathbf{p}_{iel,ipt} = \begin{bmatrix} \text{SCFAX} & 0.0 & 0.0 & 0.0 & \text{SCFMY} & \text{SCFMZ} \\ A_{st,iel} & & & & W_{y,iel,ipt} & W_{z,iel,ipt} \end{bmatrix}$$

$$W_{y,iel,ipt} = \frac{W_{y,iel}}{\sin \left(\frac{2\pi \cdot ipt}{N_{pt}} \right)} \quad iel = 1, 2, \dots, N_{el} \quad ipt = 1, 2, \dots, N_{pt}$$

$$W_{z,iel,ipt} = \frac{W_{z,iel}}{\cos \left(\frac{2\pi \cdot ipt}{N_{pt}} \right)}$$

where $A_{st,iel}$ is the cross section steel area, $W_{y,iel}$ is the section modulus for bending about the y-axis and $W_{z,iel}$ is the section modulus for bending about the z-axis.

$W_{y,iel} = W_{z,iel}$ in the present version of the program. SCFAX, SCFMY and SCFMZ are stress concentration factors for axial tension, bending about local y-axis and bending about local z-axis, respectively.

3. Stresses at the element ends are represented by the complex number

$$\sigma_{r,iel,iend,ipt}, \quad r = 1, 2, \dots, N_f \quad iel = 1, 2, \dots, N_{el} \quad iend = 1, 2 \quad ipt = 1, 2, \dots, N_{pt}$$

Time series of the stress can be written as a summation of the contributions from all response frequencies,

$$\sigma_{iel,iend,ipt}(t) = \sum_{r=1}^{N_f} \sigma_{r,iel,iend,ipt} \cdot e^{i(\omega_r t + \varepsilon_r)},$$

where ω_r is the response frequency for frequency no. r and ε_r is the phase angle for response at this frequency. The latter is drawn randomly from an even distribution between 0 and 2π .

Writing the complex number as one real component and one imaginary component we get,

$$\sigma_{r,iel,iend,ipt} = \sigma_{Re,r,iel,iend,ipt} + i\sigma_{Im,r,iel,iend,ipt}$$

We then have

$$\sigma_{iel,iend,ipt}(t) = \sum_{r=1}^{N_f} \sigma_{a,r,iel,iend,ipt} \cdot \cos(\omega_r t + \theta_{r,iel,iend,ipt} + \varepsilon_r)$$

where

$$\sigma_{a,r,iel,iend,ipt} = \sqrt{\sigma_{Re,r,iel,iend,ipt}^2 + \sigma_{Im,r,iel,iend,ipt}^2} \quad \text{and} \quad \theta_{r,iel,iend,ipt} = \text{atan} \left(\frac{\sigma_{Im,r,iel,iend,ipt}}{\sigma_{Re,r,iel,iend,ipt}} \right)$$

$r = 1, 2, \dots, N_f$ $iel = 1, 2, \dots, N_{el}$ $iend = 1, 2$ $ipt = 1, 2, \dots, N_{pt}$.

4. A time series of length T (sec.) is generated. A number of stress ranges, ($\Delta\sigma_i$, $i = 1, 2, \dots, N_{\Delta\sigma}$) must be defined, and the rain flow counting method is used for finding the number of occurrences for each cycle, $n_{i,iel,iend,ipt}$. Total number of cycles for stress range i during one year is calculated from,

$$n_{i,\text{year},iel,iend,ipt} = \frac{n_{i,iel,iend,ipt} \cdot 365 \cdot 24 \cdot 60 \cdot 60}{T},$$

and the accumulated fatigue damage is found from,

$$D_{iel,iend,ipt} = \sum_{i=1}^{N_{\Delta\sigma}} \frac{n_{i,\text{year},iel,iend,ipt}}{N_i},$$

where N_i is the number of cycles to failure for stress cycle i.

N_i is found from;

$$\log N_i = \log C + m \cdot \log \left(\Delta\sigma_i \cdot \left(\frac{t_{iel}}{t_{ref}} \right)^k \right)$$

where $\log C$, m , t_{ref} and k are SN-data for the curve segment used, t_{iel} is the wall thickness for the cross section and $\Delta\sigma_i$ is the stress range.

9. DRAG AMPLIFICATION

The drag coefficient of a riser, which is subject to vortex-induced vibrations, will increase when the oscillation amplitude increases. VIVANA calculates this drag amplification in two different ways:

Blevins, (1990):

$$\frac{C_d\left(\frac{A}{D}\right)_i}{C_d(A=0)_i} = 1 + 2.1 \cdot \left(\frac{A}{D}\right)_i \quad (30)$$

Vandiver, (1983):

$$\frac{C_d\left(\frac{A}{D}\right)_i}{C_d(A=0)_i} = 1 + 1.043 \cdot \left(\frac{2 \cdot A_{rms}}{D}\right)_i^{0.65} \quad (31)$$

where

$$\frac{C_d\left(\frac{A}{D}\right)_i}{C_d(A=0)_i}$$

is the drag amplification factor at element i.

A_i

is the response amplitude at element i.

D_i

is the diameter of element i.

$A_{rms,i}$

is the rms-value of the response at element i.

REFERENCES.

Blevins, R.D. (1990): "*Flow-Induced Vibration*" (Second Ed.). van Nostrand & Reinhold, New York, USA.

Faltinsen, O. M.(1990): "*Sea Loads on Ships and Offshore Structures*". Cambridge University Press, Cambridge, UK.

Gopalkrishnan, R. (1993): "*Vortex-Induced Forces on Oscillating Bluff Cylinders*". D.Sc. thesis, Department of Ocean Engineering, MIT, Boston.

Larsen, Carl M., Baarholm, Gro S., Passano, Elizabeth and Koushan, Kamran: "*Non-Linear Time Domain Analysis of Vortex Induced Vibrations for Free Spanning Pipelines*" OMAE2004-51404, Proceedings of 23rd International Conference on Offshore Mechanics and Arctic Engineering, Vancouver, Canada, June 2004

Lie, H, Larsen, C.M. and Vandiver, J.K. (1997): "*Vortex Induced Vibrations of Long Marine Risers; Model test in a rotating rig*" Proceedings from OMAE 1997, Yokohama

RIFLEX Theory Manual, SINTEF Report STF70 F95219, September 1995, Trondheim, Norway.

Vandiver, J. Kim (1983). "*Drag coefficients of long flexible cylinders*", In Proc. of the 15th Annual Offshore Technology Conference, Houston, TX, pp 405-410, OTC Paper No. 4490.

Venugopal, Madan (1996). "*Damping and response prediction of a flexible cylinder in a current*", Ph.D. thesis submitted to Dept. of Ocean Eng, MIT.

Vikestad, K.(1998): "*Multi-Frequency Response of a Cylinder Subjected to Vortex Shedding and Support Motions*", PhD. thesis, Department of Marine Structures, NTNU, Trondheim.

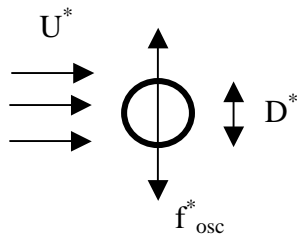
Vikestad, K, Larsen, C.M. and Vandiver, J.K. (2000): "*Norwegian Deepwater Program: Damping of Vortex-Induced Vibrations*", Proceedings from OTC 2000, Houston, TX, Paper No. OTC11998.

APPENDIX A: CORRECTION OF NON-DIMENSIONAL FREQUENCY FOR ACTUAL STROUHAL NUMBER

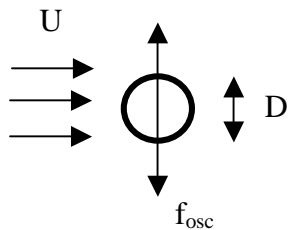
Gopalkrishnan's tests were carried out with a small cylinder. According to the standard curve for Strouhal number, as a function of Reynolds number, the Strouhal number, St_G , must have been approximately 0.2 for these tests. If we have another Strouhal number and want to apply Gopalkrishnan's results, we have to take this into account when calculating the non-dimensional frequency parameter.

General case: St^*

$$f_v = \frac{St_G U}{D} \quad (32)$$



Gopalkrishnan's case: St_G



Non-dimensional frequency

$$\hat{f}^* = \frac{f_{osc}^* D^*}{U^*} \quad (33)$$

Vortex shedding frequency

$$f_v^* = \frac{St^* U^*}{D^*} \quad (34)$$

Non-dimensional frequency

$$\hat{f} = \frac{f_{osc} D}{U} \quad (35)$$

The general case is assumed to be equivalent to Gopalkrishnan's case if

$$\frac{f_{osc}^*}{f_v^*} = \frac{f_{osc}}{f_v} \quad (36)$$

The non-dimensional frequency can now be defined from parameters in the general case:

$$\frac{f_{osc}^*}{St^* U^*} = \frac{\hat{f} \frac{U}{D}}{St_G \frac{U}{D}} = \frac{\hat{f}}{St_G} \quad (37)$$

Hence

$$\hat{f} = \frac{f_{osc}^* D^*}{U^*} \cdot \frac{St_G}{St^*} \quad (38)$$

By using this definition for the non-dimensional frequency in all operations we can use Gopalkrishnan's data directly.

If we calculate the reduced velocity from the standard definition

$$U_R = \frac{U}{f_0 D} \quad (39)$$

for a system with Strouhal number $= St^*$ that is different from St_G , and want to compare such values to values obtained from the relation (cf. Eq. 16),

$$U_R = \frac{1}{\hat{f}} \sqrt{\frac{\bar{m}+1}{\bar{m} + \frac{C_a}{C_{a0}}}} \quad (40)$$

we have to correct U_R in order to take care of the difference in Strouhal number. If we assume that the ratio f_0/f_v should be constant, the correction will be as follows

With standard Strouhal number:

$$\frac{f_0}{f_v} = \frac{\frac{U}{U_R D}}{St_G \frac{U}{D}} = \frac{1}{U_R St_G} \quad (41)$$

At a different Strouhal number:

$$\frac{f_0}{f_v} = \frac{1}{U_R St^*} \quad (42)$$

We can now define a modified U_R that will give the same ratio. This must be as follows:

$$U_R^* = U_R \cdot \frac{St_G}{St^*} \quad (43)$$

By using this definition of the reduced velocity we can compare U_R^* directly to values found from the standard relation between U_R and the non-dimensional frequency in Gopalkrishnan's experiments.